Quenching Spin Decoherence in Diamond through Spin Bath Polarization

Susumu Takahashi,[1,*] Ronald Hanson,[2,3] Johan van Tol,[4] Mark S. Sherwin,[1] and David D. Awschalom[3]

[1]*Department of Physics and Center for Terahertz Science and Technology, University of California, Santa Barbara, California 93106*

[2]*Kavli Institute of Nanoscience, Delft University of Technology, P.O. Box 5046, 2600 GA Delft, The Netherlands*

[3]*Department of Physics and Center for Spintronics and Quantum Computation, University of California, Santa Barbara, California 93106*

[4]*National High Magnetic Field Laboratory, Florida State University, Tallahassee Florida 32310*

(Dated: April 9, 2008)

We experimentally demonstrate that the decoherence of a spin by a spin bath can be completely eliminated by fully polarizing the spin bath. We use electron paramagnetic resonance at 240 gigahertz and 8 Tesla to study the spin coherence time T_2 of nitrogen-vacancy centers and nitrogen impurities in diamond from room temperature down to 1.3 K. A sharp increase of T_2 is observed below the Zeeman energy (11.5 K). The data are well described by a suppression of the flip-flop induced spin bath fluctuations due to thermal spin polarization. T_2 saturates at ~ 250 μs below 2 K, where the spin bath polarization is 99.4 %.

PACS numbers: 76.30.Mi, 03.65.Yz

Overcoming spin decoherence is critical to spintronics and spin-based quantum information processing devices [1, 2]. For spins in the solid state, a coupling to a fluctuating spin bath is a major source of the decoherence. Therefore, several recent theoretical and experimental efforts have aimed at suppressing spin bath fluctuations [3, 4, 5, 6, 7, 8, 9]. One approach is to bring the spin bath into a well-known quantum state that exhibits little or no fluctuations [10, 11]. A prime example is the case of a fully polarized spin bath. The spin bath fluctuations are fully eliminated when all spins are in the ground state. In quantum dots, nuclear spin bath polarizations of up to 60% have been achieved [12, 13]. However, a polarization above 90% is need to significantly increase the spin coherence time [14]. Moreover, thermal polarization of the nuclear spin bath is experimentally challenging due to the small nuclear magnetic moment. Electron spin baths, however, may be fully polarized thermally at a few degrees of Kelvin under an applied magnetic field of 8 Tesla.

Here we investigate the relationship between the spin coherence of Nitrogen-Vacancy (N-V) centers in diamond and the polarization of the surrounding spin bath consisting of Nitrogen (N) electron spins. N-V centers consist of a substitutional nitrogen atom adjoining to a vacancy in the diamond lattice. The N-V center, which has long spin coherence times at room temperature [15, 16], is an excellent candidate for quantum information processing applications as well as conducting fundamental studies of interactions with nearby electronic spins [16, 17, 18] and nuclear spins [19, 20]. In the case of type-Ib diamond, as studied here, the coupling to a bath of N electron spins is the main source of decoherence for an N-V center spin [15, 21]. We have measured the spin coherence time (T_2) and spin-lattice relaxation time (T_1) in spin ensembles of N-V centers and single N impurity centers (P1 centers) using pulsed electron paramagnetic resonance (EPR) spectroscopy at 240 GHz. By comparing the values of T_1 and T_2 at different temperatures, we verify that the mechanism determining T_2 is different from that of T_1. Next, we investigate the temperature dependence of T_2.

At 240 GHz and 8.6 T where the Zeeman energy of the N centers corresponds to 11.5 K, the polarization of the N spin bath is almost complete (99.4 %) for temperatures below 2 K as shown in Fig. 1(a). This extremely high polarization has a dramatic effect on the spin bath fluctuations, and thereby on the coherence of the N-V center spin. We find that T_2 of the N-V center spin is nearly constant between room temperature and 20 K, but increases by almost 2 orders of magnitude below the Zeeman energy to a saturation value of ~ 250 μs at 2 K. The data shows excellent agreement with a model based on spin flip-flop processes in the spin bath. The observed saturation value suggests that when the N spin bath is fully polarized, T_2 is limited by the fluctuations in the ^{13}C nuclear spin bath.

We studied a single crystal of high-temperature high-pressure type-Ib diamond, which is commercially available from Sumitomo electric industries. The density of N impurities is 10^{19} to 10^{20} cm^{-3}. The sample was irradiated with 1.7 MeV electrons with a dose of 5×10^{17} cm^{-3} and subsequently annealed at 900 °C for 2 hours to increase the N-V concentration [22].

Electronic spin Hamiltonians for the N-V (H_{NV}) and N centers (H_N) are,

$$H_{NV} = D[(S_z^{NV})^2 - \frac{1}{3}S(S+1)] + \mu_B g^{NV} \boldsymbol{S}^{NV} \cdot \boldsymbol{B}_0 + A^{NV} \boldsymbol{S}^{NV} \cdot \boldsymbol{I}^N, \quad (1)$$

*Electronic address: susumu@iqcd.ucsb.edu

$$H_N = \mu_B \boldsymbol{S}^N \cdot \overleftrightarrow{g^N} \cdot \boldsymbol{B}_0 + A^N \boldsymbol{S}^N \cdot \boldsymbol{I}^N, \qquad (2)$$

where μ_B is the Bohr magneton and $\boldsymbol{B}_0$ is the magnetic field. $\boldsymbol{S}^{NV}$ and $\boldsymbol{S}^N$ are the electronic spin operators for the N-V and N centers and $\boldsymbol{I}^N$ is the nuclear spin operator for ^{14}N nuclear spins. $g^{NV} = 2.0028$ [23], and $\overleftrightarrow{g^N}$ is the slightly anisotropic g-tensor of the N center. $D = 2.87$ GHz is the zero-field splitting due to the axial crystal field [23]. Due to the tetrahedral symmetry of diamond lattice, there are four possible orientations of the defect principal axis of the ^{14}N hyperfine coupling of A^N and A^{NV}. In the present case, $A^N = 114$ MHz for the $\langle 111 \rangle$-orientation and $A^N = 86$ MHz for the other three orientations [24]. For the N-V center, $A^{NV} = 2.2$ MHz for the $\langle 111 \rangle$-orientation [23]. The nuclear Zeeman energy and the hyperfine coupling between the N-V (N) center and ^{13}C and the nuclear Zeeman energy are not included here. The energy states of the N-V and N centers are shown in Fig. 1(b).

The measurement was performed using a 240 GHz continuous wave (cw) and pulsed EPR spectrometer in the electron magnetic resonance program at the National High Magnetic Field Laboratory (NHMFL), Tallahassee FL. The setup is based on a superheterodyne quasioptical bridge with a 40 mW solid state source. Details of the EPR setup are described elsewhere [25, 26]. No optical excitation was applied throughout this paper, and no resonator was used for either cw or pulsed experiments. Fig. 1(c)-(f) shows cw EPR spectra at room temperature where the magnetic field was applied along the $\langle 111 \rangle$-direction of the $\sim 0.8 \times 0.8 \times 0.6$ mm^3 single crystal diamond. The applied microwave power and field modulation intensity were carefully tuned not to distort the EPR lineshape. Five EPR spectra in Fig. 1(c) corresponding to the N center are drastically stronger than the remaining signals which indicates that the number of N centers dominates the spin population in the sample. The N EPR peaks show the slightly anisotropic g-factor g^N which gives $g^N_{\|} = 2.0024$ and $g^N_{\perp} = 2.0025 \sim 6$ and is in agreement with the reported g-anisotropy of type-IIa diamond [27]. As shown in Fig. 1(d), we also observed the much smaller N-V resonances which shows a line for the $\langle 111 \rangle$-orientation in the right side and three lines for the other orientations in the left side. An overlap of the three lines is lifted because the applied B_0 field is slightly tilted from the $\langle 111 \rangle$-direction. Based on the EPR intensity ratio between N and N-V centers, the estimated density of the N-V centers in the studied sample is approximately 10^{17} to 10^{18} cm^{-3}. EPR lineshapes of the N ($|m_S = -1/2, m_I = 1\rangle \leftrightarrow |1/2, 1\rangle$) and N-V ($|m_S = -1\rangle \leftrightarrow |0\rangle$) centers are shown in Fig. 1(e) and (f) respectively. The N center shows a single EPR line with a peak-to-peak width of 0.95 gauss. On the other hand, the N-V center shows a broader EPR line (the peak-to-peak width is 2.36 gauss) due to the hyperfine coupling between the N-V center and the ^{14}N nuclear spins. The estimated hyperfine constant is 2 MHz, in good agreement with a previous report [23].

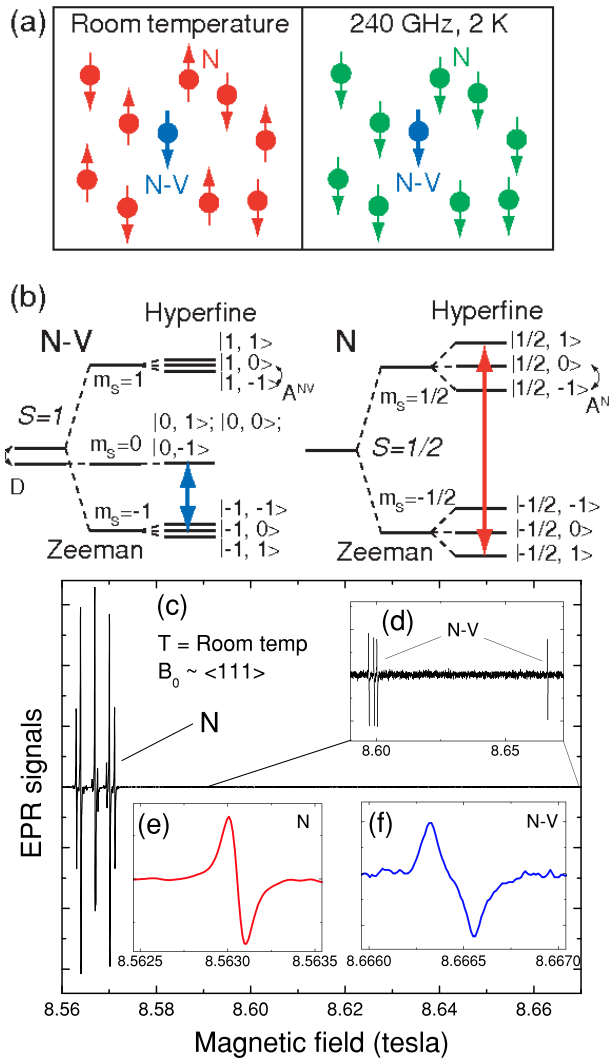

FIG. 1: (a)Spins of the N-V and N centers at room temperature and at 8.56 tesla and 2 K. At room temperature, where up and down spins are nearly equally populated, the N spin bath polarization is very small and therefore, the spin flip-flop rate is high. At 240 GHz and 2 K, the N spin bath polarization is 99.4 % and the spin flip-flop rate is nearly zero. (b)Energy states of the N-V and N centers. The energy levels are not scaled. The states are indexed by $|m_S, m_I\rangle$. Transitions indicated by solid lines are EPR peaks used to measure the spin relaxation times T_1 and T_2. (c)cw EPR spectrum at 240 GHz at room temperature when the magnetic field B_0 is applied along the $\langle 111 \rangle$-direction. No optical pump is applied. The strongest five EPR peaks around 8.57 tesla are from N centers. (d) N-V EPR peaks. The intensity ratio between the left-most N and the right-most N-V is ~ 80 which corresponds to 120:1 population ratio between N and N-V centers respectively. Other impurity centers were also observed (not indicated). (e)N centers EPR for the transition of $|m_S = -1/2, m_I = 1\rangle \leftrightarrow |1/2, 1\rangle$. (f)N-V centers EPR for the transition of $|m_S = -1\rangle \leftrightarrow |0\rangle$.

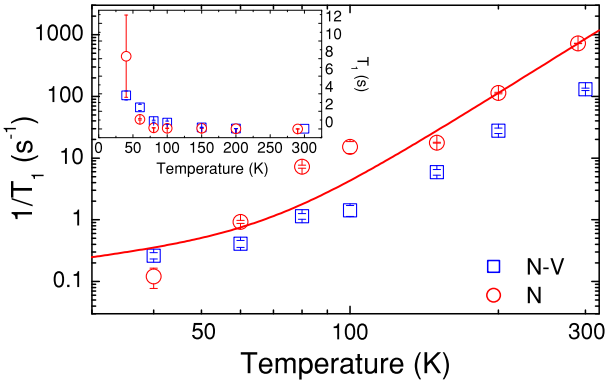

FIG. 2: $1/T_1$ for the N-V and N centers as a function of temperature. Solid lines are the best fit of the spin-orbit phonon-induced tunneling model written by Eq. 3. Inset of the graph shows T_1 versus temperature in a linear scale.

The temperature dependence of the spin relaxation times T_1 and T_2 was measured using pulsed EPR. An echo-detected inversion recovery sequence $(\pi - T - \pi/2 - \tau - \pi - \tau - echo)$ is applied for T_1 where a delay T is varied, while a Hahn echo sequence $(\pi/2 - \tau - \pi - \tau - echo)$ is applied for T_2 where a delay τ is varied [28]. The area of the echo signal decays as a function of the delay time T and 2τ for T_1 and T_2 respectively and therefore can be used to determine the relaxation times. For the pulsed EPR measurement, we used the $|m_S = -1, m_I = 0\rangle \leftrightarrow |0, 0\rangle$ transition for the N-V center and the $|m_S = -1/2, m_I = 1\rangle \leftrightarrow |1/2, 1\rangle$ transition for the N center (Fig. 1(b)).

The T_1 for both the N-V and N centers was measured from room temperature to 40 K. Below 40 K where the T_1 is longer than 10 seconds, an accurate measurement proved impractical as the drift of the superconducting magnet ($\sim$ 5 ppm/hour) becomes nontrivial on the timescale of the measurement. The T_1 is obtained by fitting a decay exponential to the recovery rate of the echo area $y_0 - ae^{-T/T_1}$. As shown in the inset of Fig. 2, the T_1 of both centers increases significantly as the temperature is reduced. For the N-V center, T_1 changes from 7.7 ± 0.4 ms to 3.8 ± 0.5 s. For the N center, T_1 increases from 1.4 ± 0.01 ms to 8.3 ± 4.7 s. To evaluate the temperature dependence of the N center, we applied a spin-orbit phonon-induced tunneling model which is independent of the strength of a magnetic field [29]. The temperature dependence is given by the following,

$$\frac{1}{T_1} = AT + BT^5, \tag{3}$$

where A and B are parameters related to Jahn-Teller energy and electron-phonon interaction [29]. From the fit, we found $A = 8.0 \times 10^{-3}$ and $B = 3.5 \times 10^{-10}$ which are in good agreement with the values in Ref. [29], and confirm a largely field-independent T_1 relaxation. The temperature dependence of the N-V center also shows similar behavior. The T_1 relaxation mechanism for the N-V center is beyond the scope of this paper [30].

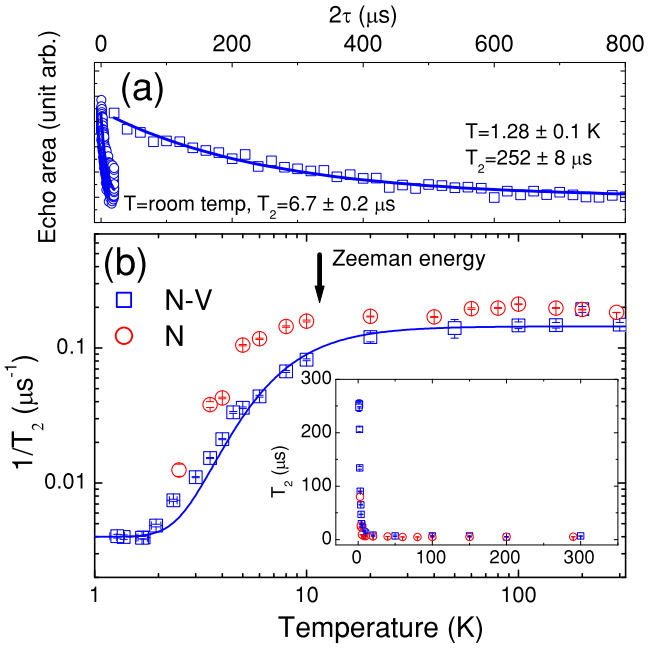

FIG. 3: (a) Echo area of the N-V center as a function of delay 2τ measured at room temperature and $T = 1.28 \pm 0.1$ K. Solid line shows the best fit by the single exponential. (b)$1/T_2$ for the N-V and N centers versus temperature. The scale of the main graph is log-log. Solid lines are the best fit using Eq. 4. The arrow shows the Zeeman energy of 11.5 K. The inset shows T_2 versus temperature in linear scale which shows a dramatic increase of T_2 below the Zeeman energy.

We also investigated the temperature dependence of the spin coherence time T_2 for the N-V center using a Hahn echo sequence where the width of the pulses (typically 500-700 ns) was tuned to maximize the echo size. Fig. 3(a) shows the decay of echo area at room temperature and at $T = 1.28 \pm 0.1$ K. These decays, which are well fit by a single exponential $e^{-2\tau/T_2}$ as shown in Fig. 3(a), show no evidence of electron-spin echo envelope modulation (ESEEM) effects from the ^{14}N hyperfine coupling [28]. This is due to the relative long microwave pulses and the nuclear Zeeman splitting at 8.5 T which is much larger than the ^{14}N hyperfine coupling of the N-V center. Between room temperature and 20 K, we observe almost no temperature dependence with $T_2 \ll T_1$, (*e.g.* the $T_2 = 6.7 \pm 0.2$ μs at room temperature and $T_2 = 8.3 \pm 0.7$ μs at 20 K). This verifies that the mechanism which determines T_2 is different from that of T_1. Below the Zeeman energy (11.5 K), T_2 increases drastically as shown in the inset of Fig. 3(b). By lowering the temperature further, T_2 increases up to ~ 250 μs at 1.7 K and doesn't show noticeable increase below 1.7 K.

At high magnetic field, where single spin flips are suppressed, the fluctuations in the bath are mainly caused by energy-conserving flip-flop processes of the N spins. The spin flip-flop rate in the bath is proportional to the number of pairs with opposite spin and thus it strongly depends on the spin bath polarization [31]. At 240 GHz

and 2 K, the N spin bath polarization is 99.4 % which almost eliminates the spin flip-flop process. This experiment therefore verifies that the dominant decoherence mechanism of the N-V center in type-Ib diamond is the spin-flop process of the N spin bath. Using the partition function for the Zeeman term of the N spins, $Z = \sum_{S=-1/2}^{1/2} e^{-\beta\mu_B g^N B_0 S}$ where $\beta = 1/(k_B T)$ and k_B is Boltzmann constant, the flip-flop rate is modelled by the following equation [31],

$$\frac{1}{T_2} \equiv C P_{m_S=-1/2} P_{m_S=1/2} + \Gamma_{res} = \frac{C}{(1+e^{T_{Ze}/T})(1+e^{-T_{Ze}/T})} + \Gamma_{res}, \quad (4)$$

where C is a temperature independent parameter, T_{Ze} is the temperature corresponding to Zeeman energy and Γ_{res} is a residual relaxation rate. We fit the T_2 data for the N-V center using the equation above. The fit was performed with the fixed $\Gamma_{res} = 0.004$ (μs^{-1}) corresponding to 250 μs. This model fit the data well as shown in the log scale plot of Fig. 3(b). $T_{Ze} = 14.7 \pm 0.4$ K obtained from the fit is in reasonable agreement with the actual Zeeman energy of 11.5 K. The result thus confirms the decoherence mechanism of the N spin bath fluctuation.

The observation of the saturation of $T_2 \sim 250$ μs also indicates complete quenching of the N spin bath fluctuation and a second decoherence source in this system. From previous studies [16, 19], the most probable second source is a coupling to the ^{13}C nuclear spin bath. In fact, $T_2 \sim 250$ μs agrees with an estimated decoherence time of ^{13}C spin bath fluctuations [16].

Finally we investigate temperature dependence of T_2 for the N center at 240 GHz. No temperature dependence of T_2 was observed in a previous pulsed EPR study at 9.6 GHz [29]. We measured the $|m_S = -1/2, m_I = 1\rangle \leftrightarrow |1/2, 1\rangle$ transition shown in Fig. 1(b) which can excite only 1/12 of the N center population while it is assumed that all N spins in this transition are on resonance [24]. The temperature dependence of T_2 therefore shows the relationship between 1/12 of the N center and 11/12 of the N spin bath fluctuation. Similar to the N-V center, we found slight change between room temperature and 20 K, *i.e.* $T_2 = 5.455 \pm 0.005$ μs at room temperature and $T_2 = 5.83 \pm 0.04$ μs at 20 K, and then a significant increase below the Zeeman energy. Eventually, T_2 becomes 80 $\pm$ 9 μs at 2.5 K. As shown in Fig. 3(b), the temperature dependence of T_2 is similar to that of the N-V center. These facts support strongly that the decoherence mechanism of the N center is also the N spin bath fluctuation.

In conclusion, we presented the temperature dependence of the spin relaxation times T_1 and T_2 of the N-V and N centers in diamond. The temperature dependence of T_2 confirms that the primary decoherence mechanism in type-Ib diamond is the N spin bath fluctuation. We have demonstrated that we can strongly polarize the N spin bath and quench its decoherence at 8 T and 240 GHz. We observed that T_2 of the N-V center saturates ~ 250 μs below 2 K which indicates a secondary decoherence mechanism and is in good agreement with an estimated coherence time dominated by ^{13}C nuclear spin fluctuations.

This work was supported by research grants; NSF and W. M. Keck foundation (M.S.S. and S.T.), FOM and NWO (R.H.) and AFOSR (D.D.A.). S.T. thanks the NHMFL EMR program for travel support.

[1] D. D. Awschalom and M. E. Flatté, Nature Phys. **3**, 153 (2007).
[2] R. Hanson et al., Rev. Mod. Phys. **79**, 1217 (2007).
[3] A. V. Khaetskii, D. Loss, and L. Glazman, Phys. Rev. Lett. **88**, 186802 (2002).
[4] I. A. Merkulov, Al. L. Efros, and M. Rosen, Phys. Rev. B **65**, 205309 (2002).
[5] R. de Sousa and S. Das Sarma, Phys. Rev. B **68**, 115322 (2003).
[6] V. V. Dobrovitski, H. A. De Raedt, M. I. Katsnelson, and B. N. Harmon, Phys. Rev. Lett. **90**, 210401 (2003).
[7] F. M. Cucchietti, J. P. Paz, and W. H. Zurek, Phys. Rev. A **72**, 052113 (2005).
[8] J. M. Taylor and M. D. Lukin, Quant. Info. Proc. **5**, 503 (2006).
[9] W. Yao, R.-B. Liu, and L. J. Sham, Phys. Rev. Lett. **98**, 077602 (2007).
[10] D. Stepanenko, G. Burkard, G. Giedke, and A. Imamoglu, Phys. Rev. Lett. **96**, 136401 (2006).
[11] D. Klauser, W. A. Coish, and D. Loss, Phys. Rev. B **73**, 205302 (2006).
[12] A. S. Bracker et al., Phys. Rev. Lett. **94**, 047402 (2005).
[13] J. Baugh, Y. Kitamura, K. Ono, and S. Tarucha, Phys. Rev. Lett. **99**, 096804 (2007).
[14] W. A. Coish and D. Loss, Phys. Rev. B **70**, 195340 (2004).
[15] T. A. Kennedy et al., Appl. Phys. Lett. **83**, 4190 (2003).
[16] T. Gaebel et al., Nature Phys. **2**, 408 (2006).
[17] R. Hanson, F. M. Mendoza, R. J. Epstein, and D. D. Awschalom, Phys. Rev. Lett. **97**, 087601 (2006).
[18] R. Hanson, V. V. Dobrovitski, A. E. Feiguin, O. Gywat, and D. D. Awschalom, Science, March 13 (2008), (10.1126/science.1155400).
[19] L. Childress et al., Science **314**, 281 (2006).
[20] M. V. Gurudev Dutt et al., Science **316**, 1312 (2007).
[21] R. Hanson, O. Gywat, and D. D. Awschalom, Phys. Rev. B **74**, 161203R (2006).
[22] R. J. Epstein, F. M. Mendoza, Y. K. Kato, and D. D. Awschalom, Nature Phys. **1**, 94 (2005).
[23] J. H. N. Loubser and J. A. vanWyk, Rep. Prog. Phys. **41**, 1201 (1978).
[24] W. V. Smith, P. P. Sorokin, I. L. Gelles, and G. J. Lasher, Phys. Rev. **115**, 1546 (1959).
[25] J. van Tol, L.-C. Brunel, and R. J. Wylde, Rev. Sci.

Instrum. **76**, 074101 (2005).
[26] G. W. Morley, L.-C. Brunel, and J. van Tol, arXiv:0803.3054.
[27] S. Zhang et al., Phys. Rev. B **49**, 15392 (1994).
[28] A. Schweiger and G. Jeschke, in *Principles of Pulse Electron Paramagnetic Resonance* (Oxford Univeristy Press, New York, 2001).
[29] E. C. Reynhardt, G. L. High, and J. A. vanWyk, J. Chem. Phys. **109**, 8471 (1998).
[30] S. Takahashi et al., (to be published).
[31] C. Kutter et al., Phys. Rev. Lett. **74**, 2925 (1995).